

## Negative-pion capture process and its chemical effects in some hydrocarbons

Atsushi Shinohara, Toshiharu Muroyama, Junichiro Shintai, Junji Kurachi, and Michiaki Furukawa  
*Department of Chemistry, Faculty of Science, Nagoya University, Chikusa-ku, Nagoya 464-01, Japan*

Taichi Miura and Yoshio Yoshimura  
*National Laboratory for High Energy Physics (KEK), Tsukuba, Ibaraki 305, Japan*

Tadashi Saito  
*Department of Chemistry and Laboratory of Nuclear Studies, Faculty of Science, Osaka University, Toyonaka, Osaka 560, Japan*

Toshiyuki Ohdaira\* and Nobutsugu Imanishi  
*Department of Nuclear Engineering, Faculty of Engineering, Kyoto University, Sakyo-ku, Kyoto 606-01, Japan*  
(Received 17 April 1995; revised manuscript received 17 July 1995)

A negative-pion capture process for several kinds of hydrocarbons was studied by the simultaneous observation of low-energy pionic x rays and  $\pi^0$  decays following the nuclear capture of pions by hydrogen. We measured the pionic x-ray intensity pattern and the pion-capture probabilities of constituent carbon and hydrogen. The x-ray intensity pattern depends on the chemical environment; a cascade calculation showed that this can be qualitatively attributed to the effects of a pion transfer from hydrogen. The pion-capture probabilities on hydrogen could be explained by a combined model involving a modified large mesomolecular model and an external transfer process. The external transfer parameter of the pion from a pionic hydrogen atom to carbon atoms was deduced to be  $\Lambda_C = 1.7 \pm 0.2$  based on the results for a series of alkanes in the condensed phase. The large difference between the pion-capture probabilities on hydrogen observed in alkanes and that in benzene can be well understood based on the proposed model.

PACS number(s): 36.10.Gv

### I. INTRODUCTION

Numerous experimental results concerning muon and pion capture in both compounds and mixtures of chemical elements evidently show that the capture ratio depends not only on the nuclear charges of the atoms concerned but also strongly on the electronic environment in the substances [1,2]. However, an understanding of the mechanism by which the valence electrons affect the pion- or muon-capture process is far from complete. The main questions remaining unanswered are the distribution of pions or muons within the molecules immediately following pion capture in the molecules, as well as the nature of a subsequent process involving the transfer of pions or muons from hydrogen atoms to heavier-Z atoms.

As for pion capture, the experimental data in this field are generally concerned with either the capture probabilities ( $W_Z$ ) on different-Z atoms (usually obtained from pionic x-ray measurements) or the capture probabilities ( $W_H$ ) on hydrogen (obtained from the charge-exchange reaction,  $\pi^- p \rightarrow \pi^0 n$ ;  $\pi^0 \rightarrow 2\gamma$ , following pion capture on hydrogen). The intensity patterns of the pionic x rays also give additional information concerning the capture mechanism.

In measuring the x rays, however, the use of strongly interacting particles such as pions has some drawbacks compared to the use of muons, because the broadening of inner levels of an exotic atom due to nuclear absorption makes

measurements of some inner-shell transitions difficult. On the other hand, the use of pions has an advantage in that pion capture on hydrogen can be easily detected through a charge-exchange reaction.

In recent years, many studies in this field have been devoted to pion capture in complex molecules [3–5]. Especially, studies concerning pion capture by organic compounds provide valuable data for investigating molecular effects, because the fraction of valence electrons relative to the total number of electrons is large in such constituent elements, and the molecule includes various atoms having the same nuclear charge but with different chemical states. So far, many authors [4–8] have separately measured either the pionic x-ray spectra or the probabilities of the pion charge exchange by hydrogen in organic compounds. This is because a thin target is inevitably necessary for observing pionic x rays lying in the low-energy range (18–50 keV); on the contrary, a bulky sample is necessary for measuring the  $\pi^0$ -decay  $\gamma$  rays.

We have constructed an apparatus which allows us to carry out simultaneous measurements of the  $\pi^0$ -decay  $\gamma$  rays and low-energy pionic x rays and have studied the pion-capture process in graphite, benzene, cyclohexane, *n*-alkanes, and polyethylene. We first describe the experimental setup and the performance of the apparatus. Next, the pionic x-ray yields for carbon in the different chemical environments are presented for the results with alkanes and benzene. In the following discussion, we propose a revised large mesomolecular (LMM) model combined with an external transfer process in order to explain the observed  $W_H$  for the alkanes. A large chemical effect observed between the

\*Present address: Electrotechnical Laboratory, Tsukuba, Ibaraki-305, Japan.

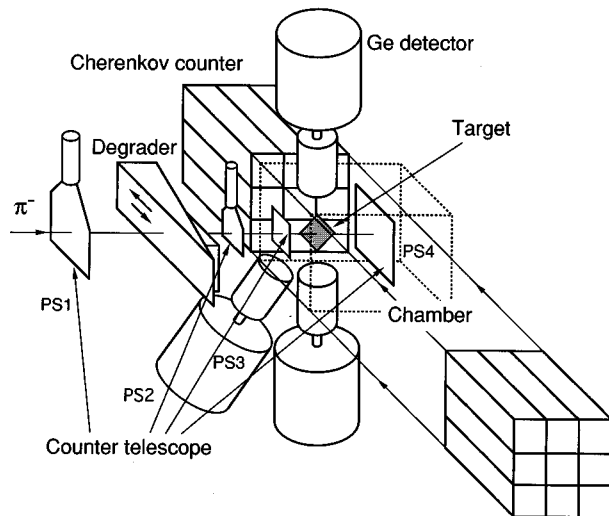


FIG. 1. Schematic view of the experimental setup installed at the  $\pi\mu$  channel of KEK-PS.

$W_H$ 's of the alkanes and benzene is also discussed based on the revised model. Finally, we discuss the chemical effects in the x-ray intensity patterns on the basis of an atomic-cascade calculation.

## II. EXPERIMENT

### A. Experimental setup

The experimental setup was installed at the  $\pi\mu$  channel of the 12-GeV proton synchrotron of the National Laboratory for High Energy Physics (KEK), Japan. The channel comprises a D4Q2D2Q lens system and has a length of 11.0 m from the production target to the sample position. The production target for the secondary beam was a Pt rod of 60 mm in length and 6 mm in diameter. The central production angle was  $147^\circ$  with respect to the primary proton beam. The details of the channel are described in [9].

The apparatus comprised an energy degrader, a collimator, a radiation shield, a defining counter system, and a measuring chamber, as shown in Fig. 1. Negative pions were slowed down by the graphite degrader so as to stop in the target. The degrader consisted of two wedge-shaped graphite plates, one of which was movable in order to vary its thickness. The thickness could be varied from 0 to 150 mm with 0.2-mm precision using a pulsed stepping motor controlled by a microcomputer. Incident and stopping pions in the sample were counted using a conventional counter telescope comprising four plastic scintillation counters [PS1, PS2, PS3, and PS4 (veto)].

The optimum conditions for the beam momentum were determined based on the beam intensity and stop-range width. The beam channel was tuned for pions having a momentum of  $p=140$  MeV/c; the momentum spread was  $dp/p=\pm 2.5\%$ . The beam size at the sample position was defined as  $4(H)\times 3(V)$  cm<sup>2</sup> by the collimator and the defining counters (PS2 and PS3 in Fig. 1). The typical incident intensity and the stop-range width [full width at half maximum (FWHM)] for the sample were approximately  $5\times 10^4$   $\pi^-/s$  and 2.8 g/cm<sup>2</sup> carbon equivalent, respectively.

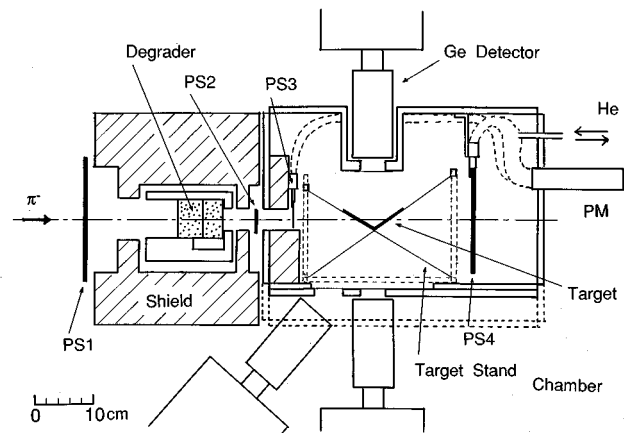


FIG. 2. Cross-sectional view of the helium-flow chamber for the measurement of organic compounds. Scintillators PS3 and PS4 (veto) were set inside the chamber and coupled with the respective photomultipliers (PM) through light guides made of optical fiber. A thin plastic scintillator of 0.5 mm in thickness was used as the PS3 counter in order to reduce the background of two  $\gamma$  rays. The windows of the chamber for Ge detectors were 10- $\mu$ m-thick aluminum foils, and the side windows for the Cherenkov counters (not shown) were 100- $\mu$ m-thick aluminum foils. Two Ge detectors were installed above and below the target at a distance of 12 cm from the beam axis. Another detector was set so as to look sideways at the target at a distance of 20 cm from it.

The pionic x rays were measured with two or three Ge detectors in coincidence with the stop events ( $1*2*3*\bar{4}$ ). Three portable low-energy photon spectrometers (LEPS) were used as detectors for measuring the x rays. The upper and lower detectors (with a 14-mm-thick crystal of 36-mm diam) were reverse-electrode-type Ge detectors manufactured by EG&G ORTEC with an energy resolution of 291 eV for 5.9-keV and 540 eV for 122-keV photons. The third detector looked at the target from the side (see Fig. 1). It was an EG&G ORTEC planar-type detector (with a 10-mm-thick crystal of 16-mm diam), which had an energy resolution of 191 eV for 5.9-keV and 485 eV for 122-keV photons.

Two coincident  $\gamma$  rays from a charge-exchange reaction,  $p+\pi^-\rightarrow n+\pi^0$ ,  $\pi^0\rightarrow 2\gamma$  (70 MeV each, 60% branching ratio), were detected using a pair of Cherenkov-detector arrays. Each array consisted of nine lead-glass Cherenkov counters having a large solid angle ( $10\times 10$  cm<sup>2</sup> in area and 38 cm in length). These arrays were also usable as a position-sensitive detector having  $3\times 3$  segments each. The specifications of the counters, as well as the  $\pi^0$  detection and analysis methods, have been described in detail elsewhere [10].

Figure 2 exhibits the cross section of the measuring chamber. The sample was set in the chamber filled with helium gas in order to avoid any disturbance from air. The pressed powder sample was a self-supporting type having a square shape of  $4\times 4$  cm<sup>2</sup>. A rectangular container [ $5.5(H)\times 7.0(V)$  cm<sup>2</sup> in area and 2.5, 5.0, or 7.5 mm in thickness] made of thin beryllium or aluminum foil was used for liquid and powder samples. The window thickness of the container was 0.2 mm for beryllium or 0.1 mm for aluminum. One or two samples were placed on a support made of aluminum

TABLE I. Comparison between the experimental correction factors and the Monte Carlo calculations for the target self-absorption. The 14.4-, 122-, and 136-keV  $\gamma$  rays are those from  $^{57}\text{Co}$ , and the 22.6-keV  $K_{\alpha,\beta}$  x rays and 88-keV  $\gamma$  ray are those from  $^{109}\text{Cd}$ . The resin is cation-exchange resin (Dowex 50W).

Substance (thickness)	Photon energy (keV)	Correction factor $\varepsilon_{\text{abs}}$	
		Experimental	Calculated
Resin (0.363 g/cm <sup>2</sup> )	14.41	0.618±0.012	0.641±0.003
	22.6	0.820±0.003	0.833±0.003
	88.03	0.896±0.015	0.913±0.003
	122.1	0.918±0.002	0.914±0.003
	136.5	0.912±0.009	0.914±0.003
Al powder (0.705 g/cm <sup>2</sup> )	14.41	0.177±0.005	0.180±0.002
	22.6	0.477±0.002	0.495±0.003
	88.03	0.886±0.013	0.887±0.003
	122.1	0.902±0.002	0.892±0.003
	136.5	0.902±0.008	0.894±0.003
TiO <sub>2</sub> powder (0.476 g/cm <sup>2</sup> )	14.41	0.100±0.004	0.094±0.002
	22.6	0.290±0.002	0.300±0.002
	88.03	0.883±0.014	0.889±0.003
	122.1	0.923±0.002	0.901±0.003
	136.5	0.922±0.008	0.904±0.003
Zn powder (1.843 g/cm <sup>2</sup> )	14.41	0.0072±0.0012	0.0061±0.0005
	22.6	0.0221±0.0002	0.0197±0.0010
	88.03	0.584±0.009	0.562±0.003
	122.1	0.811±0.002	0.725±0.003
	136.5	0.845±0.007	0.758±0.003

wire inclined by 40° relative to the beam axis, as shown in Fig. 2.

The arrangement and tuning of the electronics were done on the basis of a method described elsewhere [10]. All the data were accumulated on a computer hard disk or floppy disks through a microcomputer-based CAMAC electronic system.

### B. Performance of the experimental apparatus

The counting efficiency for pionic x rays was determined based on the detection-efficiency curve of the Ge detector obtained with calibrated point sources (supplied from LMRI, France) and corrections for a geometric factor and self-absorption in extended and bulky samples. The corrections were made using a Monte Carlo calculation (see the next section). The uncertainty in the detection efficiency was estimated to be 5.0–3.5 % in the energy range from 15 to 100 keV. The overall efficiency of the coincidence measurement was evaluated to be 0.92–0.95 within 3% error based on the delayed and singles measurements.

The energy gain of each Cherenkov counter for 70-MeV  $\gamma$  rays was calibrated with 70-MeV/c electrons. The total detection efficiency for two  $\gamma$  rays with the Cherenkov detector system was determined to be  $\varepsilon = 0.055 \pm 0.003$  from measurements for polyethylene  $[(\text{CH}_2)_n]$  samples, whose  $W_{\text{H}}$  value was known to be  $W_{\text{H}} = 1.290 \pm 0.036 \times 10^{-2}$  [8]. The event of pion capture by hydrogen in the sample was assigned based on the energy and trajectory of the  $\gamma$  rays. The  $\gamma$ -ray energy (70 MeV) was deduced by summing the energy signals of the nine counters, and the  $\gamma$ -ray trajectory

was reproduced from the detection positions of the detector pair [10]. The background two- $\gamma$ -ray signal, which originated from fast  $\pi^-$  reactions upstream and stop events in the PS3 counter, was also evaluated based on control measurements of a blank sample with a constituent similar to that of the actual sample, except for hydrogen. No interference of low-energy  $\gamma$  rays and fast neutrons was caused in this method. The  $W_{\text{H}}$  value for the sample was obtained after subtracting the background deduced from the dependence of a two- $\gamma$ -ray event on the degrader thickness and from the results of the control measurement. The detection limit for the  $\gamma$  rays could be reduced to the required low level ( $\sim 2 \times 10^{-5}/\pi^-$ ).

### C. Self-absorption correction

In spite of the use of thin targets, a correction for the self-absorption of pionic x rays in the target is necessary for a quantitative determination of the low-energy pionic x-ray intensities. We made corrections for the solid angle and self-absorption in an extended target by means of a Monte Carlo method.

The simulation included a calculation of the average solid angle subtended by a cylindrical detector at an arbitrary point [11], the generation of a point in the target by taking into account the pion-stop distribution, and a calculation of the self-absorption of the emitted photon. The self-absorption was calculated simply by using a factor of  $\exp(-\mu x)$  with a path length ( $x$ ) of the photon within the target and the photoabsorption coefficients ( $\mu$ ) [12] for the sample material. We tried two types of calculations using the total absorption

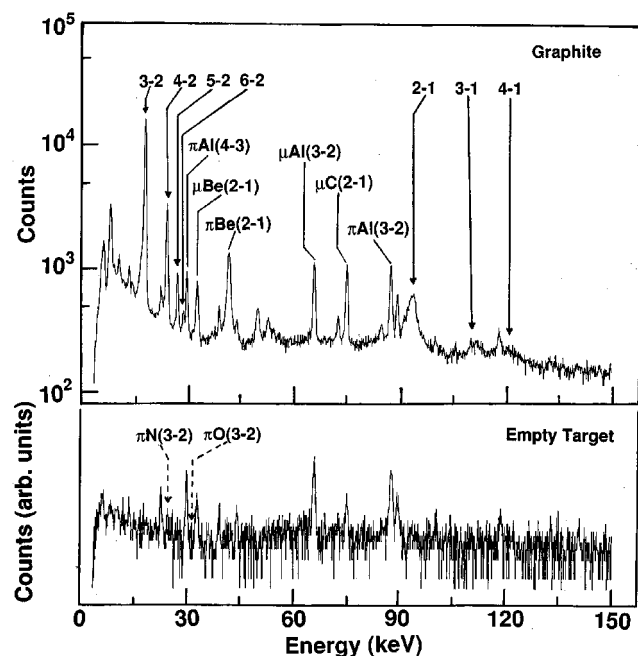


FIG. 3. Typical pionic x-ray spectra for graphite and empty target (background). The assigned x-ray lines are denoted by the principal quantum numbers relevant to the transition. The Lyman- and Balmer-series pionic x rays for carbon are observed in the upper spectrum; the lower spectrum shows no disturbance from air in the energy range.

coefficients of the photons and the coefficients without the coherent process; better results were obtained in the latter case.

The reliability of this method was examined for various materials by a comparison between the calculation and the experimental results for the known activities of  $^{57}\text{Co}$  and  $^{109}\text{Cd}$ , as shown in Table I. We can obtain the following qualitative tendency: (1) for  $Z \leq 10$ , the deviation lies within 3%; (2) for  $10 < Z \leq 20$ ; the deviation is smaller than 5% for the high-energy range ( $> 20$  keV) and larger than or about 5% for the low-energy range ( $\leq 20$  keV); and (3) for  $Z > 20$ , the deviation becomes equal to or larger than 5%. The result also shows the overall tendency of this calculation to underestimate the correction factors for high atomic numbers. As a result, this method was found to be reliable within a 3% deviation for the organic compounds in which we are interested.

#### D. Measurement of samples

We measured the pion-capture probabilities for carbon and hydrogen as well as the pionic x-ray intensity pattern of C(graphite),  $\text{C}_6\text{H}_6$ ,  $\text{C}_6\text{H}_{12}$ ,  $n\text{-C}_m\text{H}_{2m+2}$  ( $m = 5, 6, 8, 10$ , and  $15$ ), and  $(\text{CH}_2)_n$  (polyethylene). For a liquid sample, 10 or 18.5 ml of each sample was contained in an aluminum or beryllium case. The graphite sample (99.999% pure) was 13.0 g of powder contained in the beryllium case, and the polyethylene samples were 2- to 4-mm-thick sheets. An optimum pion stopping rate in the sample was selected for each sample by varying the thickness of the degrader (the typical thickness was 87 mm). The measuring time was 4–8 h and the typical numbers of incident and stopped pions were  $1.0 \times 10^8$  and  $3 \times 10^7$  per run, respectively. Measurements

were repeated more than twice for a target of the same substance but with different thicknesses (2.5 and 5 mm). The self-absorption correction of the sample was determined based on the consistency of the results for different thicknesses, and the agreement between two sets of data measured with the upper and the lower Ge detectors, in addition to experimental tests for the Monte Carlo method described above.

Figure 3 shows a typical pionic x-ray spectrum for graphite. The Lyman- and Balmer-series pionic x rays for carbon were observed. The pionic x-ray peaks of oxygen and nitrogen from air were substantially reduced. Some muonic x rays were also observed for Be and Al; the origin of the muons was attributable to the decay of pions during the flight from the PS3 to the PS4 counters.

The number of pions stopped in the sample was derived from a comparison between the stop events for the sample and the empty holder. The measurement for the empty holder includes the contribution from pions stopped or scattered in the holder itself, the counters, and the surrounding material. The effect of pions scattered in the sample itself has been determined by the comparative measurements in which the distance between the PS3 and the PS4 counters was varied to change the contribution of the scattering; the uncertainty from the effect in determining the number of stopped pions has been found to be about or less than 2% for light elements such as the present samples [13].

### III. RESULTS

#### A. Pion-capture probabilities of constituent elements

The measured x-ray intensities of pionic carbon C(3-2) and the capture probabilities on hydrogen ( $W_H$ ) are presented in the second and third column of Table II, respectively. The  $W_C$  values given by  $1 - W_H$  and the capture-per-atom ratio ( $R_H/R_C$ ) are also given in the fourth and the last column, respectively.

The errors attached to the tabulated values include the statistical errors in determining the peak areas and counting the stopped pions and do not include the systematic errors in the interest of a comparison among the compounds. The systematic error for the absolute values of the C(3-2) intensities was estimated to be 6.2% based on the uncertainties in the detection efficiency, the self-absorption correction, the coincidence-measurement loss, and the scattering effect by the samples substance. The systematic error for the  $W_H$  values was evaluated to be 5.5% from the ambiguity of the scattering effect and the uncertainty in the detection efficiency of the Cherenkov counters.

The  $W_H$  values obtained are plotted against the number of carbon atoms in the molecules together with the previous data [6,7] in Fig. 4. Chemical effects were found: a large difference between the  $R_H/R_C$  values in benzene and cyclohexane (or polyethylene) and a slight change in  $R_H/R_C$  among a series of alkanes.

#### B. X-ray intensity pattern

The intensity patterns of the Balmer series of pionic x rays are presented as intensities relative to the (3-2) transition in Table III. The errors of the tabulated values include the uncertainty of the detection-efficiency function [without

TABLE II. Pionic x-ray intensities and pion-capture probabilities for constituent atoms in alkanes and benzene. The  $W_C$  values were given by  $1 - W_H$ .  $R_H/R_C$  denotes the per-atom capture ratio of hydrogen to carbon. The attached errors in the second column included no systematic error (about 6.2%). The attached errors in the third column included no systematic error (about 5.5%).  $W_H$  values were normalized for  $W_H((CH_2)_n) = (1.290 \pm 0.036) \times 10^{-2}$  [8].

Sample	C(3-2) (per 100 stop $\pi^-$ )	Capture probabilities (%)		
		$W_H$	$W_C$	$10^3 R_H/R_C$
C(graphite)	$52.2 \pm 1.2$		100	
$n$ -C <sub>5</sub> H <sub>12</sub>	$32.7 \pm 0.6$	$1.56 \pm 0.02$	98.44	$6.61 \pm 0.08$
$n$ -C <sub>6</sub> H <sub>14</sub>	$33.4 \pm 0.6$	$1.48 \pm 0.02$	98.52	$6.45 \pm 0.08$
$n$ -C <sub>8</sub> H <sub>18</sub>	$33.4 \pm 0.6$	$1.47 \pm 0.02$	98.53	$6.61 \pm 0.08$
$n$ -C <sub>10</sub> H <sub>22</sub>	$34.0 \pm 0.6$	$1.40 \pm 0.02$	98.60	$6.46 \pm 0.09$
$n$ -C <sub>15</sub> H <sub>32</sub>	$35.0 \pm 0.7$	$1.32 \pm 0.02$	98.68	$6.26 \pm 0.09$
(CH <sub>2</sub> ) <sub><math>n</math></sub>	$33.9 \pm 1.1$	1.290	98.710	6.534
C <sub>6</sub> H <sub>12</sub>	$35.1 \pm 0.6$	$1.25 \pm 0.02$	98.75	$6.31 \pm 0.08$
C <sub>6</sub> H <sub>6</sub>	$39.8 \pm 1.0$	$0.365 \pm 0.006$	99.64	$3.66 \pm 0.11$

the systematic error (3%) from the calibrated sources], in addition to the statistical errors.

The intensity ratios for the hydrocarbons are apparently larger than those in elementary carbon (graphite). Among the hydrocarbons, the intensity ratios for polyethylene are almost equal to those of cyclohexane but are slightly larger than those for benzene. The former fact for the hydrocarbons means that the difference in the physical state for the solid and liquid phases scarcely influences the x-ray pattern. The latter fact shows that the chemical environment of the carbon atom influences the capture process of pions.

### C. Pionic x-ray yields of carbon in hydrocarbons

The pion-capture probabilities for constituent elements heavier than He in a molecule can be obtained from the pionic x-ray intensity per stopped pion and the x-ray emission yield per atom. The pionic x-ray yield is usually derived from the x-ray intensity for samples of a single element. This elemental yield, however, seems to be inadequate to determine the capture probability of each constituent in the molecule, because the x-ray intensity pattern in a molecule is different from that in a single element. In muonic atoms, the capture rate can be obtained from the sum of the x-ray intensities in the Lyman series, because the electron emission (Auger process) can be neglected in inner-shell transitions. For pionic atoms, however, this method is not applicable, because the nuclear absorption of pions changes the x-ray yields.

In the present case, the x-ray yields of pionic carbon for individual hydrocarbon compounds can be obtained from the x-ray intensities ( $I_C$ ), because the capture probability of carbon ( $W_C$ ) is equal to  $1 - W_H$ . First, in  $n$ -C <sub>$m$</sub> H<sub>2 $m$ +2</sub>, we assumed that the individual carbon atoms have the same capture rates in the molecule and introduced  $Y_C(CH_2)$  as the C(3-2) x-ray yield of carbon in the methylene group ( $-CH_2-$ ) and  $Y_C(CH_3)$  as that in the methyl group ( $-CH_3$ ). The following relation then holds for all  $n$ -C <sub>$m$</sub> H<sub>2 $m$ +2</sub>:

$$I_C/\bar{Y}_C + W_H = 1, \quad (1)$$

where

$$\bar{Y}_C = 2Y_C(CH_3)/m + (m-2)Y_C(CH_2)/m. \quad (2)$$

We determined the yields so as to be consistent among all samples by means of a least-squares method and obtained  $Y_C(CH_3) = 0.284 \pm 0.015$  and  $Y_C(CH_2) = 0.343 \pm 0.005$ . The  $Y_C(CH_2)$  value obtained from C<sub>6</sub>H<sub>12</sub> was consistent with the above value. The  $Y_C(CH)$  value for C<sub>6</sub>H<sub>6</sub> was also estimated to be  $Y_C(CH) = 0.384 \pm 0.012$ . On the other hand, the  $Y_C$  value for graphite was directly obtained as  $Y_C = 0.522 \pm 0.012$ . The x-ray yields for hydrocarbon were small compared with those for graphite, which is consistent with the previous results [14]; furthermore, the yields are different from each other among the carbon atoms in the different chemical states.

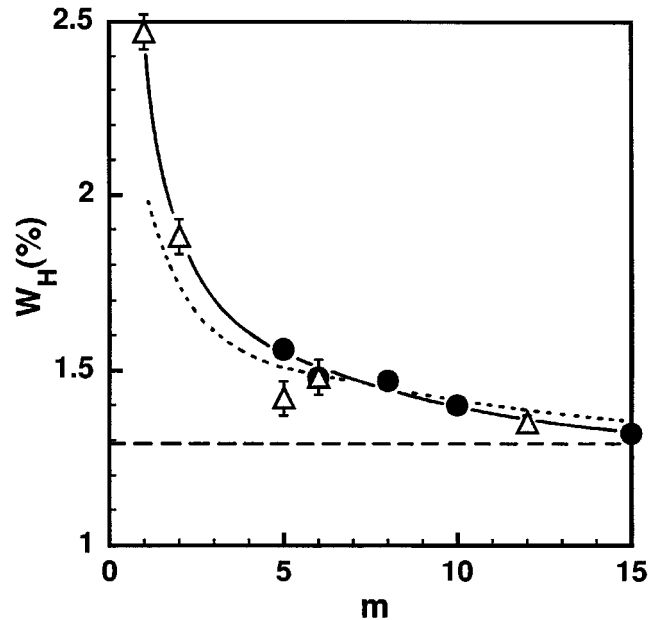


FIG. 4. Pion-capture probabilities ( $W_H$ ) in hydrogen as a function of the number of the carbon atoms ( $m$ ) in molecules. The dashed line is that for polyethylene. The closed circles are the present results and the open triangles present the previous data [6,7] normalized to the  $W_H$  value of polyethylene. The solid curve presents the fitting result for the combined model with  $\Lambda_C = 1.7$ , and the dotted curve is that without transfer ( $\Lambda_C = 0$ ).

## IV. DISCUSSION

### A. Pion-capture probabilities on hydrogen in molecules

#### 1. Combined model of an LMM model and an external transfer process

The pionic hydrogen atom ( $\pi^-p$ ) formed through pion capture in bound hydrogen becomes free from the H—Z chemical bond and moves freely in the material due to its neutral charge. In collisions with other atoms, it transfers the pion to the colliding heavier Z atoms,  $\pi^-p + Z \rightarrow \pi^-Z + p$ , or the negative pion disintegrates through a charge-exchange reaction with the proton. The former process is called “external transfer.” On the contrary, if the transfer occurs within the same molecule or the transfer to the neighboring atom proceeds by  $\pi^-$  tunneling along the H—Z bond before the  $\pi^-p$  atom becomes free, the process is distinguished from external transfer and is called “internal transfer.”

Because the lifetime of the ground state ( $1s$ ) of  $\pi^-p$  is very short ( $< 10^{-15}$  s), the external transfer phenomenon occurs only in the excited state of  $\pi^-p$ . Such a transfer process has been observed in gas mixtures of the  $H_2+X$  system [15,16] and the (hydrocarbon)+X system [7], where X indicates a series of rare gases. In this paper a discussion is given concerning the contribution of an external transfer in a condensed phase in order to explain the observed dependence of  $W_H$  on a series of hydrocarbons.

According to a phenomenological description [1,17], the capture probability of hydrogen can be expressed as

$$W_H = PQR, \quad (3)$$

where  $P$ ,  $Q$ , and  $R$  represent the probabilities of the following three processes: the pion is captured into a mesomolecular orbit localized near hydrogen, the pion makes a transition from the mesomolecular orbit to the  $\pi^-p$  atomic level, and the pion is finally absorbed by the proton.

In a previous report [3], we proposed a revised LMM model in order to formulate the  $W_H$  value in hydrogen-containing molecules. For  $Z_kH_l$ ,  $W_H$  can be written as

$$W_H = \frac{\nu(1+\sigma)a'_\gamma}{(N+\nu)(1-\sigma)Z_{\text{eff}}} \quad (4)$$

by modifying Eq. (3) in [3]. Here,  $N$  is the sum of the core electrons relevant to the capture process,  $\nu$  represents the total valence electrons,  $Z_{\text{eff}}$  denotes the effective charge of the Z atom that is equal to the sum of relevant core and valence electrons of the Z atom, and  $\sigma$  is an ionicity param-

eter which defines the displacement of the valence electrons ( $\sigma=0$  corresponds to completely covalent bonding). The parameter  $a'_\gamma$  is defined as the ratio of the rate of radiative and absorption processes to the rate of the Auger transition which would be expected if an electron was located in the hydrogen-atomic orbital, and the parameter was experimentally found to be  $a'_\gamma=0.0587$  based on data for lithium hydroxide [3]. The parameter  $a'_\gamma$  therefore includes both the contributions of internal and external transfer processes, because  $a'_\gamma/Z_{\text{eff}}$  is thought to correspond to the product of the parameters  $Q$  and  $R$  based on a comparison with Eq. (3).

We now try to combine the above model with a phenomenological treatment for the external transfer process in the gas phase [15,16]. We first approximate the parameter  $a'_\gamma$  as the product of two factors,  $a'_\gamma$  and  $R'$ , where  $R'$  is the non-transfer probability associated only with the external transfer. Equation (4) is rewritten as

$$W_H = \frac{\nu(1+\sigma)a'_\gamma}{(N+\nu)(1-\sigma)Z_{\text{eff}}} R'. \quad (5)$$

The probability  $R'$  can be expressed approximately by

$$R' = (1 + \kappa_Z C_Z) / (1 + \kappa_Z C_Z + \Lambda_Z C_Z) \approx 1 / (1 + \Lambda_Z C_Z) \quad (\text{for } \kappa \ll \Lambda), \quad (6)$$

based on a phenomenological model [15–17], where  $\Lambda_Z$  is the ratio between the pion-transfer probability from hydrogen to Z atoms and the charge-exchange probability in the collision with other hydrogen atoms,  $\kappa_Z$  is the ratio between the nuclear capture probability in the collision with Z atoms and the charge-exchange probability in the collision with other hydrogen atoms (in general, the relation  $\kappa \ll \Lambda$  holds for a heavier Z atom than hydrogen), and  $C_Z$  is the atomic ratio of the Z atom to the hydrogen atom. The  $a'_\gamma$  value should be recognized as being the probability of isolation of a  $\pi^-p$  from the Z—H bond or of absorption by the proton without experiencing an internal transfer [the latter probability is assumed to be negligibly small in Eq. (5)] and hence is determined as a particular parameter for the kind of Z—H bond.

#### 2. The $W_H$ values for alkanes

For alkanes  $n-C_mH_{2m+2}$ , we tried to reproduce the  $W_H$  observed by adjusting two parameters,  $a'_\gamma$  and  $\Lambda_Z$  ( $Z=C$ ) in Eqs. (5) and (6). The case for  $\Lambda_Z=0$  was also calculated (there is no external transfer process). In these calculations,

TABLE III. Relative pionic x-ray intensities for carbon. Averaged values are given for the alkanes studied.

Sample	(Intensities)/(3-2) (%)			
	3-2	4-2	5-2	6-2
C(graphite)	100	15.22±0.37	2.94±0.10	0.66±0.05
C <sub>6</sub> H <sub>6</sub>	100	20.14±0.47	4.15±0.29	0.80±0.12
C <sub>6</sub> H <sub>12</sub>	100	22.02±0.52	4.49±0.13	0.91±0.16
$n-C_mH_{2m+2}$	100	21.79±0.55	5.26±0.23	1.41±0.15
(CH <sub>2</sub> ) <sub>n</sub>	100	21.04±0.49	4.78±0.14	1.20±0.30

TABLE IV. Comparison between the experimental  $W_H$  values and theoretical ones calculated with the combined LMM model (see text). The calculation with  $\Lambda_C=1.70$  and  $a'_\gamma=0.140$  provided the best fit to the experimental  $W_H$  values.

Sample	Parameters used			Calc. $10^2 W_H$		Obs. $10^2 W_H^a$	
	$N$	$\nu$	$\sigma$	Trans. <sup>b</sup>	No trans. <sup>c</sup>	This work	Ref. <sup>d</sup>
<i>n</i> -alkanes							
CH <sub>4</sub>	0	8	0	2.546	1.995		2.47±0.05
C <sub>2</sub> H <sub>6</sub>	2	12	0	1.915	1.710		1.88±0.05
C <sub>3</sub> H <sub>8</sub>	4	16	0	1.710	1.596		
C <sub>4</sub> H <sub>10</sub>	6	20	0	1.603	1.535		
C <sub>5</sub> H <sub>12</sub>	8	24	0	1.537	1.496	1.56±0.02	1.42±0.05
C <sub>6</sub> H <sub>14</sub>	10	28	0	1.492	1.470	1.48±0.02	1.48±0.05
C <sub>8</sub> H <sub>18</sub>	14	36	0	1.435	1.436	1.47±0.02	
C <sub>10</sub> H <sub>22</sub>	18	44	0	1.401	1.416	1.40±0.02	
C <sub>12</sub> H <sub>26</sub>	22	52	0	1.378	1.402		1.35±0.02
C <sub>15</sub> H <sub>32</sub>	28	64	0	1.355	1.388	1.32±0.02	
C <sub>17</sub> H <sub>36</sub>	32	72	0	1.344	1.381		1.25±0.05
(CH <sub>2</sub> ) <sub><i>n</i></sub>	2	4	0	1.261	1.330	1.290 <sup>e</sup>	
Cyclohexane							
C <sub>6</sub> H <sub>12</sub>	12	24	0	1.261	1.330	1.25±0.02	1.27±0.05
Benzene							
C <sub>6</sub> H <sub>6</sub>	18	12	0	0.519		0.365±0.006	0.346±0.027
	18	12	-0.17	← 0.365		assuming $\Lambda_C=1.7^e$	
	18	12	0	0.365	→	$\Lambda_C=2.8$ , assuming $\sigma=0^f$	

<sup>a</sup>The attached errors includes no systematic error.

<sup>b</sup>Calculations with  $\Lambda_C=1.70$  and  $a'_\gamma=0.14$ .

<sup>c</sup>Calculations without the external transfer ( $\Lambda_C=0$ ).

<sup>d</sup>Taken from Petrukhin *et al.* [7] and Krumshtein *et al.* [6] renormalized to  $W_H[(CH_2)_n]$ .

<sup>e</sup>The data were normalized to  $W_H[(CH_2)_n]=(1.290\pm 0.036)\times 10^{-2}$  [8].

<sup>f</sup>See text.

$\nu$  was defined as the sum of the valence electrons associated with the C—H bond and included no valence electrons for the C—C bond;  $N$  was the sum of the valence electrons for the C—C bond and the core electrons other than the 1s electrons;  $\sigma$  was set to zero, because it is generally accepted that the C—H bond in alkanes is typical covalent bonding. The values used for individual parameters are summarized in the second through fourth columns of Table IV. The best fit of Eq. (5) to the data was obtained for  $\Lambda_C=1.7\pm 0.2$  and  $a'_\gamma=0.140\pm 0.008$  (the errors include no systematic errors). The results are presented in the fifth column of Table IV and in Fig. 4 along with the case for  $\Lambda_C=0$ . The present model calculation well reproduced the observed  $W_H$ 's, showing that the external transfer process should also exist in the condensed phase.

The obtained  $\Lambda_C$  is consistent with the previous value,  $\Lambda_C=1.6\pm 0.2$ , which was obtained from measurements for (hydrocarbon)+CCl<sub>4</sub> mixtures [7], whereas it is smaller than the value predicted for an isolated atom,  $\Lambda_C=4.6$ , obtained from H<sub>2</sub>+X systems [16], and slightly smaller than  $\Lambda=2.5$  from (hydrocarbon)+X [2]. The former result for comparison with the rare-gas systems supports the previous indication that the  $\pi^-p$  isolated from the C—H bond lies in a lower excited state compared with that from the H—H bond [7]. The latter indicates the structure effect of the carbon atom in alkanes. In our measurements, no difference was found

among cyclohexane, polyethylene, and *n*-alkanes, all hydrogen atoms of which bond to a carbon atom through the  $sp^3$  hybrid orbital.

### 3. The $W_H$ value for benzene

Here we discuss the observed large difference (Table II) between the  $R_H/R_C$  values for alkanes and benzene based on the revised LMM model including the external transfer process. A model calculation using the same values of parameters  $\sigma$ ,  $\nu$ ,  $a'_\gamma$ , and  $\Lambda_C$  as those for alkanes could not reproduce the  $W_H$  value of benzene. Therefore, in the calculation for benzene, it was assumed that the  $a'_\gamma$  value was fixed at the same value as that for alkanes ( $a'_\gamma=0.14$ ) and the  $\pi$  electrons were treated as core electrons. As a result,  $\sigma=-0.17\pm 0.06$  was obtained when the value  $\Lambda_C=1.7$  was fixed. On the other hand,  $\Lambda_C=2.84\pm 0.23$  was obtained when covalent bonding,  $\sigma=0$ , was assumed. These results are presented in the bottom lines of Table IV. It can be seen that the assumption of a constant  $\Lambda_C$  requires a displacement of 0.2 electrons from hydrogen to carbon. Such a large displacement could not be explained based on the difference in the bond nature of the  $sp^3$  and  $sp^2$  hybrid orbitals. The other assumption of completely covalent bonding for the C—H bond requires that the transfer rate be considerably influenced by the atomic state of  $\pi^-p$  or the chemical environ-

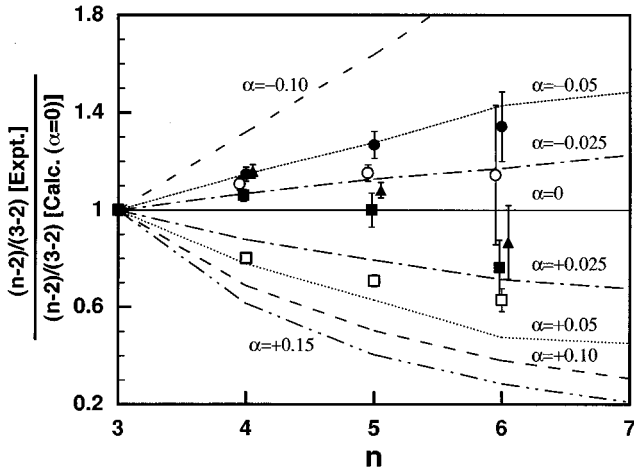


FIG. 5. Comparison between the normalized x-ray intensity pattern obtained experimentally and the predictions by a cascade calculation. The vertical axis is the intensity ratio  $(n-2)/(3-2)$  normalized to the results of the cascade calculation under the condition of  $\alpha=0$ . The lines present the cascade calculations for various values of  $\alpha$ .  $\square$ , graphite;  $\blacksquare$ ,  $C_6H_6$ ;  $\triangle$ ,  $C_6H_{12}$ ;  $\bullet$ ,  $n$ -alkanes;  $\circ$ , polyethylene.

ment of the carbon atom. Such an effect has also recently been observed in the pion-capture process for alcohols [18]. However, we cannot decide which of two assumptions is correct for explanation of the difference in  $R_H/R_C$  between alkanes and benzene. It may be a reasonable conclusion that the difference results from both of the two assumptions.

### B. Pionic x-ray intensity pattern

Figure 5 exhibits the x-ray intensity ratios normalized to the results of a cascade calculation with  $\alpha=0$  (as described below in detail) for various carbon-containing compounds, along with graphite. The observed difference in the intensity patterns should reflect the angular-momentum distribution originating in the initial process of pion capture, the refilling of surrounding electrons, and the pion being transferred from pionic hydrogen. We discuss the difference from the point of view of the chemical structure on the basis of the following cascade calculations.

We have revised the cascade code by Akylas and Vogel [19] in order to apply it to the pionic cascade by including competition of strong nuclear absorption with radiative and Auger transitions. In the initial atomic states  $(n, l)$ , from which the cascade calculation starts, the pionic-atom levels were assumed to have the population

$$P(l) \propto (2l+1)\exp(\alpha l) \quad \text{for } 0 \leq l \leq n-1 \quad (7)$$

for an orbital angular momentum of  $l$ , where  $\alpha$  is a parameter used to modify the statistical distribution. We employed a simple formula [Eq. (7)] in order to survey the tendency of the x-ray intensity ratios relative to the angular-distribution change, although more sophisticated distributions have been studied in order to consider the relation between the electronic structure and the captured-pion distribution [5,20]. In the present calculation, the cascade calculation was started at  $n=18$  under the conditions of the Auger and nuclear absorp-

tion processes described in [13]. Instantaneous refilling was assumed for the  $K$ - and  $L$ -shell electrons for all compounds and graphite. The nuclear absorption widths  $\Gamma_{1s}=2.96$  keV,  $\Gamma_{2p}=1.0$  eV, and  $\Gamma_{3d}=1.5 \times 10^{-5}$  eV were used for the  $1s$ ,  $2p$ , and  $3d$  levels in pionic carbon atoms, respectively [14]. The lines in Fig. 5 were calculated for various  $\alpha$  values and normalized to those with  $\alpha=0$ . One can see that the calculations with  $\alpha=-0.02$  to  $-0.05$  well reproduce the results for alkanes,  $\alpha=0$  for benzene, and  $\alpha=+0.05$  for graphite, except for the values of  $(6-2)/(3-2)$ . The negative value of  $\alpha$  corresponds to an enhancement of the low-angular-momentum part, whereas  $\alpha>0$  indicated an enhanced population of the high-angular-momentum level part. In pionic atoms the enhanced population of the low-angular-momentum levels (corresponding to  $\alpha<0$ ) also leads to a decrease in the x-ray yields, because nuclear absorption increases with decreasing angular momentum of an orbital pion. Therefore, the result for the intensity pattern is consistent with the tendency of the obtained x-ray yields.

The angular distribution of orbital pions is considered to be affected by the following restrictions: (i) a limitation of the angular momentum brought in by a captured pion, (ii) a restriction caused by the existence of a large mesomolecular state [21,22], and (iii) the contribution of a pion with low angular momentum by an intramolecular transfer from a  $\pi^-p$  atomic state.

The maximum angular momentum ( $l_{\max}$ ) of captured pions is equal to  $(n-1)$  for free atoms; it may become smaller than  $(n-1)$  for constituent atoms in a molecule due to the above (i) and/or (ii) restrictions. The  $l_{\max}$  value brought in by a pion can be estimated as being the product of the maximum impact parameter and the maximum linear momentum of a pion to be captured [13,23]. For carbon atoms in the compounds studied, the  $l_{\max}$  value corresponds to the bond length between carbon atoms, assuming that the maximum impact parameter is equal to half the bond length. As a result, we obtained the following order for  $l_{\max}$ :  $l_{\max}(\text{alkane}) > l_{\max}(\text{graphite}) > l_{\max}(\text{benzene})$ , because their bond lengths are 0.154, 0.142, and 0.140 nm, respectively [24]. This order is, however, inconsistent with the tendency of the angular-momentum distribution deduced from the  $\alpha$  parameter based on the cascade calculation.

The angular-momentum distribution of pions captured by carbon atoms bonding to hydrogen atoms is distorted to the low-angular-momentum range due to the contribution of low-angular-momentum pions transferred from pionic hydrogen. On the basis of this process (iii), the low-angular-momentum part in the distribution should increase along with the number of hydrogen atoms bonding to the carbon. The present result is qualitatively explained by this process. This is considered to be mainly due to internal transfer, because external transfer accounts only for a small fraction of the capture probability, and the initial capture ratio of hydrogen is estimated to be approximately 0.27 for  $-\text{CH}_3$  and 0.20 for  $-\text{CH}_2-$  based on the present model calculation (see Sec. IV A) with  $a'_\gamma=1$ . It is necessary for quantitatively understanding the effects to further discuss them while taking into account both the atomic-cascade calculations and the combined LMM model calculations proposed here. However, the very small values of the intensity ratios for graphite

may be affected by the chemical structure, as discussed concerning the capture of muons in graphite, diamond, soot, and boron nitride [25].

## V. SUMMARY AND CONCLUSIONS

The pion-capture process in graphite, benzene, polyethylene, cyclohexane, and a series of alkanes was studied by measuring the pionic x rays and  $\pi^0$  decays simultaneously. Chemical effects were observed for the pion-capture probabilities on hydrogen of hydrocarbons and the x-ray intensity patterns of pionic carbons. The pionic (3-2) x-ray yields per captured pion were determined for individual carbon atoms lying in different chemical environments in hydrocarbons. These yields are useful for analyzing the capture probabilities in more complicated organic compounds.

A combined model of the modified LMM model and an external transfer process was proposed in order to explain the  $W_H$  values for hydrocarbons. The calculations provided a quantitative agreement with the observed values as well as a definite piece of evidence concerning the external transfer process in the liquid phase. The transfer parameter was deduced to be  $\Lambda_C = 1.7 \pm 0.2$  for the pion transfer from  $\pi^- p$  to C for alkanes. It was found from a comparison with the previous results that the value reflected the difference in the atomic state of  $\pi^- p$  and the structure effect of the relevant carbon atom. A systematic study of such a chemical effect found in the transfer parameters should provide important information concerning the microscopic mechanism of the transfer process.

The intensity ratios  $[(n-2)/(3-2)]$  for hydrocarbons are larger than those for graphite, and the ratios for alkanes are slightly larger than those for benzene. This effect could be qualitatively understood as being due to a contribution of pionic hydrogen. The entire capture mechanism, including an inner transfer process, will be quantitatively discussed after analyzing the x-ray intensity patterns and accumulating the  $a'_\gamma$  values for various chemical systems.

## ACKNOWLEDGMENTS

This work was performed under the Visiting Researchers' Program of the National Laboratory for High Energy Physics (KEK) of Japan. We would like to express our gratitude to Professor K. Nakai, Professor K. Takamatsu, Professor T. Ohshima, Professor S. Iwata, and Professor I. Fujiwara for their interest and encouragement during this work. We also wish to thank the staff of the Instrument Development of the School of Science of Nagoya University and the Mechanical Engineering Center of KEK, who partly constructed the measuring chamber and setup. We are also grateful to the operating crew of the 12-GeV proton synchrotron and the beam-channel group for providing the pion beam. We appreciate the helpful advice of Dr. J. Imazato and Dr. Y. Kawashima concerning the use of the beam channel. We are thankful for the help given by H. Matsushita, M. Saito, T. Sato, and K. Takesako. One of the authors (A.S.) was provided with support by Grants-in-Aid for Scientific Research (No. 01740334 and No. 02854070) from the Ministry of Education, Science, and Culture of Japan.

- 
- [1] L. I. Ponomarev, *Ann. Rev. Nucl. Sci.* **23**, 495 (1973).  
 [2] D. Horváth, *Radiochim. Acta* **28**, 241 (1981).  
 [3] N. Imanishi, S. Miyamoto, Y. Takeuchi, A. Shinohara, H. Kaji, and Y. Yoshimura, *Phys. Rev. A* **37**, 43 (1988).  
 [4] D. F. Jackson, C. A. Lewis, and K. O'Leary, *Phys. Rev. A* **25**, 3262 (1982).  
 [5] D. Horváth, K. A. Anoil, F. Entezami, D. F. Measday, A. J. Noble, S. Stanislaus, C. J. Virtue, A. S. Clough, D. F. Jackson, J. R. H. Smith, and M. Salomon, *Phys. Rev. A* **41**, 5834 (1990).  
 [6] Z. V. Krumshtein, V. I. Petrukhin, V. E. Risin, L. M. Smirnova, V. M. Suvorov, and I. A. Yutlandov, *Zh. Éksp. Teor. Fiz.* **65**, 455 (1973) [*Sov. Phys. JETP* **38**, 222 (1974)].  
 [7] V. I. Petrukhin, V. E. Risin, I. F. Samenkova, and V. M. Suvorov, *Zh. Éksp. Teor. Fiz.* **69**, 1883 (1975) [*Sov. Phys. JETP* **42**, 955 (1976)].  
 [8] M. R. Harston, D. S. Armstrong, D. F. Measday, S. Stanislaus, P. Weber, and D. Horváth, *Phys. Rev. A* **44**, 103 (1991).  
 [9] K. H. Tanaka, Y. Kawashima, J. Imazato, M. Takasaki, H. Tamura, M. Iwasaki, E. Takada, R. S. Hayano, M. Aoki, H. Outa, and T. Yamazaki, *Nucl. Instrum. Methods A* **316**, 134 (1992).  
 [10] N. Imanishi, Y. Takeuchi, K. Toyoda, A. Shinohara, and Y. Yoshimura, *Nucl. Instrum. Methods A* **261**, 465 (1987).  
 [11] L. Wielopolski, *Nucl. Instrum. Methods* **143**, 577 (1977).  
 [12] Wm. J. Veigele, *At. Data Tables* **5**, 51 (1973).  
 [13] A. Shinohara, M. Furukawa, T. Saito, H. Baba, T. Miura, and N. Imanishi, *Nucl. Instrum. Methods B* **84**, 14 (1994).  
 [14] K. O'Leary and D. F. Jackson, *Z. Phys. A* **320**, 551 (1985).  
 [15] V. I. Petrukhin, Yu. D. Prokoshkin, and V. M. Suvorov, *Zh. Éksp. Teor. Fiz.* **55**, 2173 (1968) [*Sov. Phys. JETP* **28**, 1151 (1969)].  
 [16] V. I. Petrukhin and V. M. Suvorov, *Zh. Éksp. Teor. Fiz.* **70**, 1145 (1976) [*Sov. Phys. JETP* **43**, 595 (1976)].  
 [17] D. Horvath, *Phys. Rev. A* **30**, 2123 (1984).  
 [18] A. Shinohara, T. Muroyama, J. Shintai, E. Taniguchi, T. Saito, T. Miura, N. Imanishi, Y. Yoshimura, and M. Furukawa, *Hyperfine Interact.* **84**, 569 (1994).  
 [19] V. R. Akylas and P. Vogel, *Comp. Phys. Commun.* **15**, 291 (1978).  
 [20] F. J. Hartmann, H. Daniel, W. Neumann, G. Schmidt, and T. von Egidy, *Z. Phys. A* **341**, 101 (1991).  
 [21] S. S. Gershtein, V. I. Petrukhin, L. I. Ponomarev, and Yu. D. Prokoshkin, *Usp. Fiz. Nauk* **97**, 3 (1969) [*Sov. Phys. Usp.* **97**, 1 (1969)].  
 [22] H. Schneuwly, V. I. Pokrovsky, and L. I. Ponomarev, *Nucl. Phys.* **A312**, 419 (1978).  
 [23] C. J. Orth, M. E. Schillaci, J. D. Knight, L. F. Mausner, R. A. Naumann, G. Schmidt, and H. Daniel, *Phys. Rev. A* **25**, 876 (1982).  
 [24] *CRC Handbook of Chemistry and Physics*, edited by D. R. Lide, 73rd ed. (CRC, Boca Raton, FL, 1992).  
 [25] H. Schneuwly, M. Boschung, K. Kaeser, G. Piller, A. Ruetschi, L. A. Schaller, and L. Schellenberg, *Phys. Rev. A* **27**, 950 (1983).